REVIEW OF AERONAUTICAL FATIGUE INVESTIGATIONS IN JAPAN DURING THE PERIOD JULY 2007 TO MAY 2009

Edited by
Hiroyuki Terada
Japan Aerospace Technology Foundation

and

Nobuo Takeda
The University of Tokyo

For Presentation at the 31st Conference of
the International Committee on Aeronautical Fatigue

Rotterdam, The Netherlands, 25-26 May 2009

Contents

page

12.1 INTRODUCTION 12/4

12.2 LIFE EVALUATION ANALYSIS 12/5

12.2.1 Problems of Laboratory Tests for Durability Evaluation of Full-Scale Structures 12/5

12.2.2 Structural Reliability Evaluation Method Based on Bayesian Possibility Networks 12/6

12.3 FATIGUE IN METALLIC MATERIALS AND COMPONENTS 12/7

12.3.1 Property for Fatigue Crack Propagation of Friction Stir Welded 2024-T3 Aluminum Alloy 12/7

12.3.2 Effect of Surface Finish on Fatigue Strength of Friction Stir Welded Butt Joint in 2024-T3 Aluminum Alloy 12/9

12.3.3 Fatigue Life Prediction of Small Notched Ti-6Al-4V Based on the Theory of Critical Distance 12/12

12.3.4 Strength of Mar-M247/IN-718 Dissimilar Metals Joint Under Creep-Fatigue and Thermo-Mechanical Fatigue Loadings 12/13

12.4 FATIGUE IN COMPOSITE MATERIALS AND COMPONENTS 12/15

12.4.1 Fatigue Simulation for Ti/GFRP and Ti/CFRP Laminates by Using Cohesive Elements 12/15

12.4.2 Evaluation of Crack Suppression Method for Foam Core Sandwich Panel with Analyses and Experiments 12/16

12.4.3 A-VaRTM for Primary Aircraft Structures 12/17

12.5 FULL-SCALE TESTING 12/18

12.5.1 XP-1/C-X Full Scale Strength Test 12/18

12.5.2 Aging Aircraft Research Program with Retired Revenue-Service Passenger Airplane 12/19

12.5.3 Development and Full Scale Static Test of Full Scale Low-Cost Composite Wing Demonstrator with VaRTM Process 12/21

12.6 STRUCTURAL HEALTH MONITORING 12/23
12.6.1 Detection of Arrested Crack for Foam Core Sandwich Structures Using Optical Fiber Sensors Embedded in a Crack Arrester 12/23
12.6.2 Development of SHM System to Evaluate De-bonding in Composite Adhesive Structures 12/25
12.6.3 Development of Aircraft Impact Damage Detection System Using Optical Fiber Sensor Networks 12/26
12.6.4 Full-Field Damage Detection System for Composite Structures Using Pulse-Laser Generated Lamb Waves 12/28

12.7 AIRCRAFT ACCIDENT INVESTIGATION 12/29
12.7.1 Aircraft Accident Investigation and Aircraft Serious Incident Investigation 12/29

12.8 ICAF DOCUMENTS DISTRIBUTED BY JAPAN DURING 2007 TO 2009 12/30

ACKNOWLEDGEMENTS 12/30

TABLES AND FIGURES 12/31

(Last Page 12/53)

12.1 INTRODUCTION

Hiroyuki Terada, National Delegate, Japan Aerospace Technology Foundation

This review summarizes the papers on the study of aeronautical fatigue and related topics conducted in Japan during June 2007 to April 2009.

The papers were contributed by following organizations:

Japan Aerospace Exploration Agency (JAXA)
Japan Aerospace Technology Foundation (JAST)
Technical Research and Development Institute, (TRDI) MOD
Japan Transport Safety Board (JTSB)
Mitsubishi Aircraft Company
Kawasaki Heavy Industries, Ltd. (KHI)
Fuji Heavy Industries, Ltd. (FHI)
IHI Corporations
Japan Transport Safety Board (JTSB)
The University of Tokyo
Nagaoka University of Technology
Tohoku University and Osaka City University

Before describing the research activities, the author would like to introduce the general activities on aircraft development program in Japan during 2007 to 2009.

(1) Progress of R & D of aircraft:

- The development of MRJ (Mitsubishi Regional Jet) aircraft is progressing on schedule, expecting its maiden flight in 2011 and service flight in 2013.
- C-X (liftoff weight 120ton), the cargo airplane and XP-1 (liftoff weight 80ton), the patrol airplane are almost final stage of development. Both aircraft are developed under the spec of Ministry of Defense. XP-1 made the maiden flight in September, 2007 (see, Figure 12.1, below) and C-X is now under examination of static strength of airframe structures.

(2) Aircraft accident/incident investigation:

The body for aircraft accident and serious incident investigation was reorganized from Aircraft and Railways Accident Investigation Commission (ARAIC) to Japan Transport Safety Board (JTSB) and reinforced its function in October, 2008. The JTSB covers the accident investigation of air, railways and marine. Based on the investigation results, it

became to be able to issue recommendations directly to the parties concerned, such as government, transportation companies, and so on.

12.2 LIFE EVALUATION ANALYSIS

12.2.1 Problems of Laboratory Tests for Durability Evaluation of Full-Scale Structures

Hiroyuki Terada* and Takao Okada**

* Japan Aerospace Technology Foundation

** Japan Aerospace Exploration Agency (JAXA)

The problems of the following issues on the evaluation of damage tolerant characteristics of the full scale structure from laboratory tests results or computational analysis were discussed. The content is to be published in Ref. 1.

- On the problems of boundary condition among laboratory tests, computed results obtained by simplified models and full-scale fatigue tests, sufficient attention should be paid when to estimate fatigue life of fastener joint structures from the laboratory test results.
  * The simplified laboratory tests tend to lead to erroneous results because of side edge effect, clamping conditions or misalignment of loading axis. For example, Figure 12.2 shows the difference of failure mode of the fastener joint specimen with and without side edge treatment.
  * We have to aware that satisfactory results on the squeezing effect of the rivet joint by computer analysis are not obtained today. We have to take account the effect of out-of-plane compressive stress by squeezing the rivet on the nucleation and propagation of the crack emanating from the rivet holes as shown in Figure 12.3.
  * Also, we have to aware that the fatigue tests sometimes lead to wrong results, even if it was conducted by using a part of the full size structures. The case of the development of Comet aircraft is an example. Fatigue test conducted using a partial fuselage structure fixed to the rigid wall gave longer fatigue life than actual operation life.
- Effect of initial flaws to be introduced for the full-scale damage tolerant tests was also discussed. The authors recommend the following distribution equation on the numbers and size of initial flaws based on the data obtained from JAL accident caused by MSD in 1985.

$$f(t) = A_0 \frac{0.18t^{-0.82}}{0.66} \exp\left(-\frac{t^{0.18}}{0.66}\right)$$

f(t): distribution function

A_0: Severity factor ($0 < A_0 < 1$),

t: normalized flaw length, $t = a/p$ a: flaw size, p : fastener pitch

References

1) H. Terada, and T. Okada, Problems of Laboratory Tests for Durability Evaluation of Full-Scale Structures, to be published in Int. J. Fatigue, 2009.

12.2.2 Structural Reliability Evaluation Method Based on Bayesian Possibility Networks

Seiichi Ito, Sunao Sugimoto and Takao Okada

Japan Aerospace Exploration Agency (JAXA)

Bayesian Networks (BN) is the method of expressing with directed graph the causal relationship of the factor which constitutes a system, and presuming an uncertain factor using the acquired information. The method is called probability propagation, the belief network, or the probability network. BN has been developed since the 1980s as one domain of the intelligence system which enables rational decision making also under environment with much uncertainty. Its' application is advanced in various fields, such as medical analysis, system control, an information society. However, there is almost no example of application to the structure or the material field. In a structural design, its operation and maintenance, etc., it is a future necessary condition to take in the analysis tools treating uncertainty. Therefore, BN serves as effective analysis and an evaluation tool to these problems.

The evaluation tool to structural reliability is studied as the first step for applying BN to the structure and material field. Although the prior amount of subjectivity to a probability factor can be introduced in BN, the objective phenomenon as a probability event is dealt with to updating information. However, in structure reliability assessment, as many examples show, the role of engineering judgment which a subjective factor plays cannot be disregarded. So, in this research, in order to take the flexibility of information into consideration, the conventional BN was extended to treat possibility theory. That is, the BN method of the structure integrity evaluation was built, which enables information propagation of subjective probability. These outlines are shown in Fig.12.4(a). Arrows in Fig.12.4(a) express the communication of information of objective and subjective probability, and a nodes show the uncertain parameters.

In the Bayes theory which constitutes the foundations of BN, all the causes of a certain phenomenon are considered as mutually exclusive. That is, the cause by which there is no duplication is dealt with. However, the boundary of a cause is not clear and there is much ambiguous environment which overlaps mutually actually. Dempster and Shafer[1)] gave

probability to the subset which accepts this duplication, named basic probability, and systematized integration of the degree of possibility measure as subjective probability. The possibility measure has the character excluding additively from the probability principle. In this research, the possibility measure was taken in to BN and it was applied to the problem of structural reliability assessment.

Fig. 12.4(b) summarizes the application advantage of this extended BN analysis method using possibility theory to reliability evaluation of aging aircraft structure. An aging deterioration factor is roughly divided into three fields. They are uncertain factors, such as stress, environment, and material. Actually, there is correlation among these uncertain factors. Therefore, the joint probability in consideration of correlativity is required of the reliability assessment of aging structure. When construction of a correlation model is impossible, the statistical independence of a factor is assumed. On the other hand, the BN method can take correlativity into consideration. As for this method which can take in the subjectivity of a factor in the process of evaluation, the scope of reliability assessment spreads further.

References

1) Shafer, Glenn; *A Mathematical Theory of Evidence*, Princeton University Press, 1976.

12.3 FATIGUE IN METALLIC MATERIALS AND COMPONENTS

12.3.1 Property for Fatigue Crack Propagation of Friction Stir Welded 2024-T3 Aluminum Alloy

Takao Okada*, Motoo Asakawa**, Toshiya Nakamura* and Shigeru Machida*

* Japan Aerospace Exploration Agency (JAXA)

** Waseda University

Friction Stir Welding (FSW) is a relatively new weld process with the capability of welding high strength aluminum alloys. From a point of reduction of production cost and structural weight, FSW is expected to apply aircraft primary structure as an alternative to rivet joint. However, the recent regulation for damage tolerance and fatigue evaluations of aircraft structure requires understanding the location of probable fracture origin and fatigue crack growth property. Especially, it is important to investigate relationship between fatigue crack growth property of FSW panel and residual stress on the panel, because fatigue crack growth property is affected by residual stress around the weld line. In this reason, many researchers

have investigated the effect of residual stress on crack growth property[1, 2]. But their studies do not evaluate the effect of inclined angle of FSW weld line to direction of crack growth.

This research describes experimental results of fatigue crack growth test in order to clarify property for fatigue crack growth of FSW panel. The effects of residual stress on crack growth rate and redistribution of residual stress during crack growth were investigated. Additionally, the effect of inclined angel of weld line on crack growth rate and direction of crack growth were discussed.

Sheets of 2024-T3 with 2mm thickness were joined by FSW butt joint. Specimens have FSW of inclined angles of 0 or 30 degree to the direction of applied stress. Width and length of the specimen are 400 and 1,000 mm, respectively and the starter notch is introduced at the center. The specimens are subjected to cyclic loading with R = 0.1 and stress amplitude is 50 MPa. Test frequency is 5 Hz. Crack length was measured by CCD and the scale. Residual stress field was measured by the hole drilling method. Furthermore, residual stress redistribution caused by the crack propagation was observed by strain gages located in front of notch.

The peak value of residual stress in longitudinal direction, about 300 MPa, was found on weld line. Residual stress outside of the weld line was apparently smaller than that in weld line. And the residual stress in transverse direction was smaller than that in longitudinal direction by one order of magnitude.

The da/dN-ΔK curve of the FSW specimen shown in Fig. 12.5 indicated that crack propagation rate was accelerated by the tensile residual stress when the crack tip located around the weld line. After the crack tip ran through the weld line, the crack propagation rate gradually became close to that for base material. The relationship between redistribution of longitudinal stress and crack length shows that tensile stress were redistributed in front of the crack tip after the crack tip ran through the weld line. This tensile stress accelerated crack propagation rate of the crack crossing the weld line.

Comparison of crack path between the FSW specimen for 0 degree weld line and that for 30 degree shows that direction of crack growth was not affected by its inclined angle. Regardless of weld line angle, the crack grew perpendicular to the loading direction. Next, the relationship between crack length and angle of maximum principle stress in front of the notch is investigated. The direction of maximum principle stress is inclined to the weld line in case the crack tip is located near the line. If the maximum principal stress is a dominant factor for the direction of crack growth, the crack path has inclined angle. But actual crack path is mostly perpendicular to the weld line. This result indicated that the maximum principle stress

is not the primary factor for the direction of crack growth. The direction of the maximum stress amplitude seems to be a primary factor.

Crack propagation rate measured by inclined angle of 0 degree is almost same as that measured by the angle of 30 degree. It is supposed that this result is caused by cancel of crack opening stress for FSW specimen, because the maximum tensile residual stress, equal to 300 MPa, is apparently higher than the applied maximum stress, 55.6 MPa. Therefore da/dN-ΔK_{eff} curve of base material was evaluated using equation of the stress intensity range ratio, U, suggested by Schijve[3]. However, da/dN-ΔK of FSW and da/dN-ΔK_{eff} of base material did not coincide, even if crack tip was located on weld line. It implied that crack opening stress for each weld line angle is not completely canceled by the tensile residual stress. Then the crack opening stress of base material and that of FSW specimen for 0 degree weld line is measured by using extensometer. As shown in Fig. 12.6, the crack opening stress of the FSW specimen is apparently lower than that of the base material. But it is not zero. And it is confirmed that by using these crack opening stress, da/dN-ΔK_{eff} curve of both specimens well coincide.

Now we are conducting the test with specimens which have weld line of inclined angle of 45 degree to evaluate the effect of more declined weld line on crack growth rate.

References

1) Sato, H., Yamada, Y., Tanoue, Y. and Sakagawa, T.: Fatigue and Crack Propagation Properties of Friction Stir Welded Lap Joint and Panel, Proceedings of the 23th International Symposium on Aeronautical Fatigue, 08-10 June 2005, Hamburg, Germany, pp. 645-656.

2) Pacchione, M., Werner, S. and Ohrloff, .N.: Design Principles for Damage Tolerant Butt Welded Joints for Application in the Pressurized Fuselage, Proceedings of the 24rd symposium of the International Committee on Aeronautical Fatigue, 16-18 May 2007, Naples, Italy, pp.224-240.

3) Schijve, J.: Some Formulas for the Crack Opening Stress Level, Engineering Fracture Mechanics, 14 (1981), pp. 461-465.

12.3.2 Effect of Surface Finish on Fatigue Strength of Friction Stir Welded Butt Joint in 2024-T3 Aluminum Alloy

Takao Okada*, Shigeru Machida*, Motoo Asakawa** and Toshiya Nakamura*

* Japan Aerospace Exploration Agency (JAXA)

** Waseda University

Friction Stir Welding (FSW) invented by TWI in 1991 is relatively novel joining technique and there are many research activities for evaluation of properties for FSW. Its

application spreads in many structures such as automobiles, trains, rockets, ships and so on. For commercial aircraft, FSW is firstly applied to normal category aircraft in 2006 and its application to transport category aircraft is planed by other company. Therefore the way to comply with damage tolerance requirement for FSW structure is one of the intensive research activities[1, 2)].

In case of FSW joint, the microstructure in its joint is different within the cross section. This heterogeneous feature may change the crack nucleation site of its joint. The burr, the tool mark and the LOP become the crack origin. And the surface treatment of the FSW joint reduces or removes the effect of these factors and may change the location of crack origin. In this research, fatigue test of FSW joint is conducted to investigate the effect of several types of surface treatment on the fatigue property.

Specimen with tangentially blended fillets is used for the fatigue test. Specimens are cut out from the FSW panel so that welding direction is perpendicular to the loading direction and the weld line locates at the center of the specimen. Four types of surface finish (Table 12.1) are used to evaluate the effect of surface finish on the crack nucleation site and the fatigue life for the FSW joint. The specimens are subjected to cyclic loading with R=0.1 and f=10Hz. Three kinds of the maximum stress, 200, 250 or 300MPa are used in this research. The test is conducted at room temperature.

Figure 12.7 shows the S-N data for the FSW specimen. The test results for the base material with as received surface condition are also shown in the figure. This figure shows that the fatigue property for as weld specimen is apparently lower than that for the base material. The specimen fractured about 170,000 cycles at the maximum stress of 200MPa, while the base material indicates the run-out (2,000,000 cycles) at 250MPa. Most of the specimen fractured at a vicinity of the burr. In the other case, the LOP becomes the crack nucleation site. The average fatigue cycles for both surface grinding specimen shows about one order longer than that for the as weld specimen. But one specimen only reaches the run-out in this test and then the fatigue property of the FSW joint for the condition is not as same as that of the base material. The crack origin of the specimen which obtains lowest fatigue life looks like a crevice located inside of the specimen. Other specimens fractured at the end point of the gauge length or at the grinding mark by the mechanical grinding process. The fatigue performance of the top surface polished specimen is even lower than that of the as weld specimen at the maximum stress of 250MPa. Same as one of the as weld specimen, the LOP is the crack origin in this case. The fatigue cycles of the both surface polished specimen spreads widely. The shortest fatigue life is the same order of magnitude as the fatigue life for as weld specimen, while the longest fatigue life is greater than the 2,000,000cycles which is

considered as the run-out cycles for the base material. In case shorter fatigue life is obtained, the origin was a particle. On the other hand, the fatigue cycle is longer than the run-out, the fatigue crack starts from the inside of the specimen.

Several types of fracture surface are observed and some types of discontinuity states are identified depending on the surface finish. The tool mark near the burr and the LOP are considered as the origin for the as weld specimen. Next, the feature of the crevice observed for both surface grinding specimen is apparently different from that observed for the fatigue surface. It locates about 2mm away from the center of the welding line and within the track of the tool pin. Therefore this crevice seems to be a tunneling which is induced during the welding process. Based on these result, the burr near the tool mark, LOP and a crevice can be the crack origin also for the as weld specimen.

Based on the results, the burr, the tool mark and the LOP are the primary discontinuity states affecting the fatigue life for as weld specimen in this welding condition. The size in thickness direction for the burr, the tool mark and the LOP are about 0.45mm, 0.05mm and 0.15mm respectively. It is not big enough compared to an initial flaw size usually used to the damage tolerant design (e.g. 1.27mm). Their distribution along the welding line makes them critical to the fatigue property. In addition, the crevice induced by the welding process is needed to be considered if it exists. The crevice size is 1.45mm and is comparable to the initial flaw size.

For both surface grinding specimen, the tool mark and the LOP are removed and the mechanical grinding mark becomes a discontinuity state affecting the fatigue life. Roughness of grinding mark, Ra, is 25μm in this case and is smaller than discontinuity states identified for as weld specimen. Therefore the longer fatigue life is obtained.

Two types of discontinuity states, the particle and the crevice, are observed for both surface polished specimen, if the LOP is removed. The size of the particle is about 0.01mm and is same order of the grinding mark. Then the particle on the surface becomes the origin, because the grinding mark is removed. The crevice observed for both surface polished specimen is located 5.0mm away from the center of the welding line and is outside of the track of the tool pin. Then the origin is not a flaw induced by inadequate welding process. This seems to be formed by the accumulated loading.

References

1) Lemmen, H. J. K., Alderliesten, R. C., Homan J. J., and Benedictus, R.: Fatigue Crack Initiation Behaviour of Friction Stir Welded Joints in Aluminum Alloy, Proceedings of the 24th International Symposium on Aeronautical Fatigue, 16-18 May 2007, Naples, Italy, pp. 147-162.

2) Sato, H., Yamada, Y., and Tanoue, Y.: Improvement of Crack Propagation Properties of Friction Stir Welded Panels, Proceedings of the 24th International Symposium on Aeronautical Fatigue, 16-18 May 2007, Naples, Italy, pp. 163-171.

12.3.3 Fatigue Life Prediction of Small Notched Ti-6Al-4V based on the Theory of Critical Distance

Yoichi Yamashita, Hiroshi Kuroki, Masaharu Shinozaki
IHI Corporation

The high cycle fatigue (HCF) of gas turbine engine rotor blades and stator vanes remains a principal cause of failures in aircraft engines. HCF failure can result from vibration, caused by unsteady aerodynamic loads, or other fluctuating loads. And rotor blades and stator vanes are often damaged by collision with pebble, sand, and other debris ingested into the engine during take-off, landing and other conditions, which is called Foreign Object Damage (FOD). It may result in the small damage in the leading or trailing edges of airfoils. Furthermore, such damage reduces the fatigue strength of the material. Therefore, FOD-induced HCF is one of the significant themes in fatigue problems of aircraft engine component. In these view points, notched fatigue problem is important to investigate the effects of FOD on fatigue strength. In this study, it is focused to investigate the estimating method for small notched fatigue strength of forged Ti-6Al-4V which is materials of fan and compressor forward stages rotor blades and stator vanes. The estimating method is studied by using the theory of the critical distance (TCD) and fatigue test results.

In analytical study, the estimating method for high cycle fatigue life of notched Ti-6Al-4V specimens using TCD was investigated. The TCD applied to fatigue problems assumes that fatigue damage depends on the stress field distribution in the vicinity of the stress concentrator. Critical distance stress is defined as the average stress in the material characteristic length L. L is calculated as following equation, where ΔK_{th} is the range of the threshold value of the stress intensity factor and $\Delta\sigma_w$ is the plain fatigue limit.

$$L = F\frac{1}{\pi}\left(\frac{\Delta K_{th}}{\Delta\sigma_w}\right)^2$$

Critical distance stress is calculated by L and notch-tip stress distribution (σ_y) using following equation, where σ_m is mean stress and ρ and D is notch tip radius and depth.

$$\sigma_{ave} = \int_0^L \sigma_y \cdot 2\pi \cdot (R-x)dx \Big/ \int_0^L 2\pi \cdot (R-x)dx$$

$$\sigma_y = \frac{A\sigma_m}{2\sqrt{2}}\left[\left(\frac{\rho}{r}\right)^{1/2} + \frac{1}{2}\left(\frac{\rho}{r}\right)^{3/2}\right] + (K_t - A)\cdot\sigma_m$$

$$K_t = 1 + 2\left(\frac{D}{\rho}\right)^{1/2} \quad , \quad A = \frac{-\sqrt{2}(1-Kt)R^2}{\left(X + \sqrt{2}R^2\right)}$$

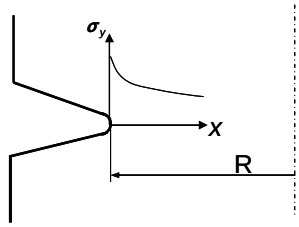

In the experimental study, very small notched round bar tension-compression fatigue tests have been conducted with forged Ti-6Al-4V material to investigate the effect of notch radius and notch depth on fatigue strength of the material. Notch radius is varied as 0.05, 0.2mm and notch depth is varied as 0.1, 0.3 and 0.5mm as shown in Figure 12.8. And stress ratio effect on fatigue strength also investigated to taking into account of residual stress. The fatigue tests shows that the larger notch radius gives the increase of fatigue strength and the larger notch depth gives the decrease of fatigue strength as shown in Figure 12.9.

Figure 12.7 also shows comparison between predicted life with TDC and fatigue test data. The predicted life is composed fatigue crack initiation life and fatigue crack growth life. Fatigue crack growth life is calculated based on the stress intensity factor taking into account of the stress concentration in the vicinity of the notch-tip and Paris' type crack growth property of Ti-6Al-4V material used. It has been found that there exists the good correlation between critical distance stress and crack initiation life of notched round bar tensile specimen. Therefore, fatigue life of Ti-6Al-4V material with various notch radius and notch depth can be predicted from the relationships between the critical distance stress and fatigue crack initiation life.

Further study of predicting FOD-induced HCF life were conducted with above mentioned fatigue life prediction method based on critical distance approach and residual stress effects on notched fatigue life of Ti-6Al-4V material. Minimum fatigue life for FOD-induced HCF life is proposed taking into account of the following factors; (1) FOD depth (notch depth) (2) Residual stress (3) Notch radius.

This study is conducted under the contract with New Energy and Industrial Technology Development Organization (NEDO) as a part of the civil aircraft basic technology program of Ministry of Economy, Trade and Industry (METI).

12.3.4 Strength of Mar-M247/IN-718 Dissimilar Metals Joint Under Creep-Fatigue and Thermo-Mechanical Fatigue Loadings.

M. OKAZAKI*, M. SAKAGUCHI* and M. SEKIHARA**

* Nagaoka University of Technology

** Hitachi Co. Ltd. , Hitachi 317-8511, Japan.

Dissimilar metals joint has been requested for advanced hybrid structures at high temperatures: e.g., so-called “BLISC” component consisting of blade and disc. Once the hybrid structures are successfully developed, they are expected to make a significant contribution to improve thermal efficiency of advanced gas turbines. In these hybrid structures, however, thermal stress which is induced by mismatches in thermal expansion coefficient and thermal conductivity between two (or more than two) base materials is a critical issue. Thus, it is inevitable to know the basic knowledge on high cycle fatigue, low cycle fatigue under creep-fatigue interaction and thermo-mechanical fatigue. In this work, the high temperature strengths of the friction welded dissimilar welded joint between the cast polycrystalline Mar-M247-LC and the forged IN-718 alloys (M247/IN718), during the low cycle and thermo-mechanical fatigue loadings, have been investigated, in comparison with those of the base metals.

The present dissimilar superalloys joint, M247/IN718, were fabricated by friction welding. Many primary tests had been carried out to optimize the welding condition, where the fabrication variables were; rotation speed of base metals, preheating time, compression normal stress to induce frictional heating, duration time of compression stress, upset pressure, and upset clearance, upset hold time, and the post weld heat treatment. From the M247/IN718 joint, the solid cylindrical M247/IN718 specimens were extracted. Low cycle fatigue (LCF) and thermo-mechanical fatigue (TMF) tests were carried out for both the welded joints and their base materials, according to the test program summarized in Table 12.2. Through the experiments, special attentions were paid to the similarities and dissimilarities between the LCF and TMF behaviors, and to those between the base materials and the joints.

The experiments clearly demonstrated that the lives of the dissimilar joints were significantly influenced by the test conditions and loading modes. Not only the lives themselves but also the failure positions and mechanisms were sensitive to the loading mode (see Fig. 12.10): in the LCF test under F-F cycling the final failure was taken place on the MM247 side far apart from the welded interface, associated with the crack propagation mode on crystallographic slip planes; in the TMF tests under both the OP and IP conditions they were on the Mar-M247 side, associated with the crack propagation mode along the dendritic boundaries; and in the LCF tests under both the tension hold and S-S waveforms they were on the IN-718 side beneath the welded interface, associated with the intergranular fracture mode.

These fracture behaviors depending on the loading modes and test conditions was discussed, based on the visco-elastic-plastic finite element method (FEM) analysis of the

welded joint. Here, an emphasis will be put on the roles of both the stress triaxiality along the specimen gauge section and the heat affected zone developed near the interface during the loading period: the both can induce a creep cavitation and intergranular fracture.

12.4 FATIGUE IN COMPOSITE MATERIALS AND COMPONENTS

12.4.1 Fatigue Simulation for Ti/GFRP Laminates by Using Cohesive Elements

Takumasa Yamaguchi*, Tomonaga Okabe*, Tatsuro Kosaka**

* Tohoku University

** Osaka City University

Hybrid laminates made of polymer matrix composite plies with metal sheet are called Fiber metal laminates (FML). In this study, a new numerical approach for the fatigue damage progress of the FML is presented. The layer-wise finite element with cohesive element are used to predict the fatigue damage progress of split, transverse crack and delamination. Four-node cohesive elements are introduced to express the 0° ply splitting and transverse crack. Eight-node cohesive elements are inserted to ply interfaces to represent the delamination. Then, the most important character of this model is that the proposed simulation introduces a damage-mechanics concept into the degradation process in cohesive elements in order to express the damage progress due to the cyclic loading. This enable us to address the complicated fatigue damage process observed in the FML. We applied this model to the Ti/GFRP laminates and compared the simulated results with the experimental data reported in the reference[1] (Fig. 12.11). We confirmed that this model could reproduce the fatigue damage process in the FML. The effects of parameters of cohesive element on Ti crack growth and delamination profile were also investigated. Ti crack growth rate was strongly associated with the delamination profile in the vicinity of the crack tip.

The same numerical procedure was also applied to Ti/CFRP laminates. The damage growth rates and damage patterns in experiments[2] were also well reproduced by the present numerical simulation (Fig. 12.12).

References

1) H. Nakatani, K. Osaka, T. Kosaka, Y. Sawada and T. Okabe：JCOM-37 Conf. Proc., (2008), pp. 230-234.

2) D. A. Burianek, S. M. Spearing：Engineering Fracture Mechanics, 70 (2003), pp. 799-812.

12.4.2 Evaluation of Crack Suppression Method for Foam Core Sandwich Panel with Analyses and Experiments

Yasuo Hirose*, Go Matsubara*, Hirokazu Matsuda*, Fumihide Inamura*, and Masaki Hojo**

* Kawasaki Heavy Industries, Ltd. (KHI)

** Kyoto University

The effect of a new type of a crack arrester was already presented in the ICAF 2007 symposium. In the previous presentation, fracture toughness test results were mainly described. This report describes the experimental validation through fatigue crack propagation tests under the mode I type and the mode II type loading conditions.

The concept of the crack arrester is to install the dissimilar material with higher stiffness on the crack propagation path in order to reduce energy release rates at the crack tip. This concept is shown in Fig.12.13. Analytical results on the energy release rate at the crack tip are shown in Fig.12.14. Here, the energy release rates were calculated and compared between with and without the crack arrester under mode I type loading condition as an example. In this figure, “Normalized energy release rate” is defined as a ratio between the energy release rate with the crack arrester and that without the arrester (using the same crack length). Distance L is also defined as the length between the leading edge of the crack arrester and the crack tip. Through these analyses, a considerable reduction of the energy release rates at the crack tip was confirmed in the FE analyses as the crack tip approached the crack arrester. This reduction of the energy release rate at crack tip was occurred owing to the load redistribution between foam core area near the crack tip and the arrester leading edge. Stress distribution of σ_{yy} is shown in Fig.12.15. This figure indicates that the stress singular field near the crack tip is decreased owing to the load redistribution. As for the mode II type loading, the similar result was obtained.

The fracture toughness tests and fatigue crack propagation tests were conducted under mode I type loading and mode II type loading in order to verify the effect on the crack arrester. Fatigue crack propagation tests under mode I type loading and mode II type loading are shown in Fig. 12.16 and Fig. 12.17, respectively. These results indicate that the relationship between the crack propagation rate, da/dN, and the distance from the leading edge of the arrester to the crack tip, L, for the specimen with the crack arrester. The crack propagation rate abruptly decreased beyond L = 15 mm for the mode I type loading and L = 10 mm for mode II type loading owing to the decrease in the energy release rate at the crack tip by the crack arrester shown in Fig.12.14.

Through these activities, the effect of the crack arrester was analytically predicted and experimentally evaluated. The validation of the crack arrester concept through the subcomponent level test article and inspection technologies for the suppressed crack near the crack arrester are further subjects of our research.

12.4.3 A-VaRTM for Primary Aircraft Structures

Morimasa Ishida
Mitsubishi Aircraft Corporation

Advanced Vacuum-assisted Resin Transfer Molding (A-VaRTM) process for Carbon Fiber Reinforced Plastics has been developed by Mitsubishi Heavy Industries, Ltd. aiming for application on aircraft primary structures with Toray Industries, Inc. Newly designed fabric and toughened resin system developed by Toray have been introduced for A-VaRTM. Comparable mechanical properties with Pre-preg material for aircraft structures are realized. The maturity of fabrication processes, the design concepts and the analysis methodology have been verified by several structural test including full-scale vertical stabilizer box strength test. A full- scale test specimen representative of regional jet type aircraft vertical stabilizer box was fabricated by using automated pre-forming process to achieve high productivity and hot compaction process to improve product quality. The maximum length, width and height of the full-scale vertical stabilizer box specimen were approximately 5.5m, 1.2m and 0.4m respectively as shown in Figure 12.18. The specimen consists of CFRP co-bond skins, CFRP spars, CFRP ribs and wing-to-body metal fittings. All CFRP parts had been fabricated with A-VaRTM technology. Each skin panel had single curved surface and aggressive ply-drop-off with 25:1 ramp ratio. Maximum thickness was approximately 10mm in the skin at the root. We confirmed that the full- scale test specimen had been fabricated without any large defects by A-VaRTM technology prior to strength test. Static strength test was conducted with an assumed critical design load case that is combination of bending and torsion. This test has been supported by Japan Aerospace Exploration Agency (JAXA). Test set-up is shown in Figure 12.19. The test was successfully conducted and the design concept and analysis methodology have been verified by test-theory correlation between analytical and practical strains and the behavior of the specimen. Strain distribution obtained from FEM analysis is shown in Figure 12.20.

12.5 FULL-SCALE TESTING

12.5.1 XP-1/C-X Full Scale Strength Test

T. Okazaki
Air Systems Research Center, Technical Research and Development Institute (TRDI), Japan Ministry of Defense

TRDI has been promoting a joint development program of the next-generation maritime patrol aircraft (XP-1) (Figure 12.21) and the next-generation cargo transport (C-X) (Figure 12.22). XP-1 is the successor of P-3C aircraft currently operated by Japan Maritime Self-Defense Force, and C-X is the one of C-1 by Japan Air Self-Defense Force. The contractor of the development program is Kawasaki Heavy Industries Ltd.

XP-1 has following characteristics of the airframe structure.

- Main wing: Low-wing arrangement fitted with the main landing gear which is stored into the fuselage
- Tail wing: Conventional form
- The fuselage is designed to secure the space for equipment and crew's working area.

C-X has following characteristics of the airframe structure.

- Main wing: High-wing arrangement for installing freights
- Tail wing: T-tail form
- The fuselage has the large-scale freight door in the after section.
- Main landing gear storage: Bulge form to secure the freight room

This joint development of XP-1 and C-X contributes to the life-cycle cost reduction by sharing the design technique, equipment, and airframe structure (part of the cockpit, outside part of the main wing and the horizontal tail).

The FSST (Full Scale Static Test) articles of XP-1 and C-X were delivered to evaluate the static strength of the airframe structure in 2006, and the FSFT (Full Scale Fatigue Test) article of XP-1 was delivered in 2007. The FSFT article of C-X is under manufacturing as of JFY 2008. Each article is neither painted nor equipped with any instruments because of unnecessity for the evaluation.

The FSST consists of the limit load tests and the ultimate load (1.5times the limit load) tests. It is to demonstrate static strength of airframe by simulating a variety of design loads, such as maneuver, gust, and landing loads, using lots of actuators controlled synchronously.

The FSFT consists of the durability test and the damage tolerant test, both of which are conducted for two life-times of spectrum loading for validation.

12.5.2 Aging Aircraft Research Program with Retired Revenue-Service Passenger Airplane

Shigeru Machida and Takao Okada
Japan Aerospace Exploration Agency (JAXA)

JAXA received one airframe of retired Model YS-11A-500 shown in Figure 12.23 from Japan Airline (JAL). The original model YS-11 aircraft is a turboprop airliner which was developed and manufactured by the Nihon Aircraft Manufacturing Corporation (NAMC). Its general characteristic and performance are listed in Table 12.3. The certification basis of YS-11 is CAR 10 dated March 28, 1955. The 182 aircrafts, including the prototype aircrafts, were manufactured by 1973 in total. In Japan, all YS-11 aircrafts for commercial usage were retired by the end of December 2006 because of the installation requirement of the Traffic Alert and Collision Avoidance System (TCAS).

The primary structures of Model YS-11 were designed based on fail-safe concept. The fatigue strength evaluation was done by safe-life evaluation method. Full-scale fatigue tests were conducted with main wing test article including center wing structure and fuselage test article separately. Scatter factor for safe-life evaluation was determined based on the assumption of structural fatigue life as log-normal distribution and usage of the typical standard deviation value in the UK at that time. As a result, 6.3 and 7.5 were determined as scatter factors for main wing structure and fuselage structure, respectively. Since the target of its initial operational life was 30,000 flight hours and flight cycles, 189,000 cycles for main wing structure and 225,000 cycles for fuselage structure were used in the fatigue tests in order to verify initial operational life. In 1983, the supplemental reviewing has been conducted on airframes of YS-11 aircrafts and SID for YS-11 was developed. As the results of above reviewing and evaluation, eight structural elements were determined to be inspected additionally and initial inspection period, interval of repeated inspections and inspection methods were established. The result of the review was presented at the 16th ICAF symposium in 1991[1)].

The retired airframe had accumulated 57,273 flight cycles and 57,002 flight hours and had experienced almost twice of the initial operational life and supplemental inspection by the SID. From technical point of view, the importance of the retired airframe is clear because of its history and the completeness of technical and maintenance documents.

The purposes of the long-term research plan are to establish the method and procedure for fatigue and damage-tolerant (DT) evaluation for aging aircraft and to create the guideline of procedure for showing compliance with fatigue and DT evaluation

requirements. For example, the FAA Advisory Circular AC25.571-1C has many items which need specific compliance methods. Table 12.4 shows the items to be determined that solutions. Guideline for compliance methods of the requirements for fatigue evaluation, widespread fatigue damage evaluation and continued airworthiness are major part of the results of the long-term research activities.

In order to obtain information of the retired airframe, such as actual damage and maintenance and loading history, the database has been established as a first stage. The SQ cards issued during the dock maintenance for the airframe is selected to be compiled into a database. Two types of the dock maintenance, a C check and an overhaul are established for this aircraft. The interval for the C check and the overhaul for YS-11A are less than 1,000 flight hours and less than 10,000 flight hours, respectively. It is confirmed that the airframe experiences 61 C checks and 6 overhauls were conducted before its retirement. Following items are decided to be included in the database: SQ card No., Maintenance facility location, Maintenance date, Maintenance type, ATA No., Zone No. Job No., Priority and Title and content of action on SQ Card. Types of damage are identified by the title and the content and are included in the database. By using the flight log, total flight cycles, total flight time and usage period are planed to add. The checkbox whether the action is based on SID or not is also considered to add. The flight log is also decided to be compiled into a database to review the flight profile such as the cruise altitude, the flight time, the cruise weight and etc. of this aircraft. From the log, the flight date, the block out time, the takeoff, the landing and the block in time and the place for departure and arrival are compiled. In addition, following information is also added to the database in case there are described: the cruise weight and altitude (pressure and feet), the outside temperature, indicated air speed and time when these data are obtained.

To investigate procedures of disassembling the structures, visual inspection and teardown inspection, a trial of teardown inspection on left main wing was conducted. Comparison of damage with maintenance record, fatigue strength of coupons with actual corrosion damage and investigation of rivet joint were expected as an output for the first stage research activities.

During the preliminary research activities, it was aroused that a definition of words and terminology from research point of view are needed to express defects on airframe including damage and corrosion by visual inspection. About 200 keywords used in the title on SQ card are identified from the database. And some of them are recognized as same meaning, although sentences or the language used are different from each other. The keywords, “lost” and “missing”, “loose” and “sticky” and “nick” and “scratch” are

examples. Then the grouping of keywords is conducted for ease of identifying the feature of each kinds of damage. On the other hand, corrosion damage is only described as "corrosion" and it is not categorized as described in the FAA advisory circular 43-4A. It is identified that difference of corrosion type affects the fatigue life. And corrosion criticality in structural integrity depends on the components [2)]. Therefore, identifying the type of corrosion will be conducted in the detailed inspection planned in near future.

References

1) T. Shiohara, et al, "AGING REVIEW OF THE YS-11 AIRCRAFT", Proceedings of the 16th ICAF Symposium, 22-24 May 1991, Tokyo Japan, pp. 175-193.
2) T. Mills, K. Honeycutt, S. Prost-Domasky and C. Brooks, "Corrosion Modeling and Life Prediction Supporting Structural Prognostic Health Management", Proceedings of the 24th ICAF Symposium, 16-18 May 2007, Naples Italy, p. 91-108.

12.5.3 Development and Full Scale Static Test of Full Scale Low-Cost Composite Wing Demonstrator with VaRTM Process

Yoshiyasu Hirano, Yuichiro Aoki, Yutaka Iwahori, Yosuke Nagao
Japan Aerospace Exploration Agency (JAXA)

In recent years, advanced composite such as graphite/epoxy composites are planned to be widely adopted for new generation commercial aircraft in order to reduce the weight, the maintenance cost and the running cost. Although composite materials have been successfully introduced to primary structures of aircraft, the raw material price is still 5-10 higher than conventional aerospace-grade aluminum[1)]. The manufacturing costs are also higher. Vacuum assisted resin transfer molding (VaRTM) method which is a composite manufacturing process, is one of the candidates to achieve cost reduction. Therefore, a development project of 6m span VaRTM wing box have been conducted by Aviation Program Group and Advanced Composite Center of JAXA since 2004[2)]. Objectives of this project are to demonstrate VaRTM wing box and to make clear the technical issues of VaRTM procedure. This wing structure is assumed a 30 passenger civil aircraft. The demonstrator was developed by step-by-step approach based on a building block approach. As a final step of this project, a practical applicability is assessed by full scale wing box assembling and subsequent full scale static and fatigue tests. At the moment, the project has successfully finished the full scale static strength test of 100% DLL (Design Limit Load). In this paper, the developing and manufacturing difficulty of a large size and complex shape structure with high quality by VaRTM process are discussed and some technical suggestions are given to overcome them.

In order to achieve the fabrication of full scale integrated wing box structure, the manufacturing process development has been started from manufacturing trial of small component. Then the manufacturing issues of large and complex integrated structure were extracted by making the size of trial target bigger. (See Figure 12.24) As a final step of manufacturing process development, a lower wing panel with integral spar and T-shape stringers was fabricated as an experimental demonstrator which contains every technical component to be solved before manufacturing of 6 m full-scale wing box structure. To take advantage of VaRTM process, skin, spars and stringers are fabricated as an integral one-shot molding except for secondary bonding of intercostals for rib connecting. External size of this panel is 2.1 m span and 1.4 m chord length, and the lower skin panel has contour form of radius approximately 7 m in order to simulate main wing cross section. For the evaluation of resin impregnation during process, this structure has three step ply drops off from root to tip, and thick sections with pad of additional plies around the maintenance holes and intersection corners between skin and spar. The thickest section is about 10 mm. There are run-out sections of stringer for evaluating the effect of this discontinuous on the resin impregnation. As a result, several quality instabilities in the manufacturing were found by visual inspection, such as incomplete resin impregnation in the thick region of corner where is skin/spar intersection, deformation of stringer web, surface wrinkle in the ply drop region and spring-in deformation at the spar corners. In order to overcome these problems, manufacturing process, layout of resin distribution medium, position of resin inlet/outlet, characteristics of resin viscosity, and cure cycles are carefully improvement by performing several times manufacturing trial of sub-component structure.

In response to these results of experimental demonstrator, the full scale 6m wing box demonstrator was successfully manufactured and assembled with modified manufacturing process. The wing box upper and lower skin panels, the front and rear main spars, and ribs are fabricated minimizing the number of mechanical fasteners needed to assemble the wing box. The wing box was designed to withstand loads associated with the flight conditions of 2.5G up-bending. The practical applicability has been verified by performing the full scale static test for 100% design limit load (DLL) of flight condition. The experimental flame for full scale test was prepared and the wing box was fixed inside of the flame. The loads are introduced to wing box through 4 hydraulic actuator/load cell assemblies. (see Figure 12.25) The hydraulic actuator control system, Aero ST produced by MTS, is adopted to control the loading. The several data acquisition systems for measuring strain, strain distribution, deformation and AE counts are adopted. 349 channels of strain gages and 12 displacement

gages are mounted on the outside and inside the wing demonstrator to measure the strain and deformation behavior.

As a result of full scale static test, the highest strain observed in the edge of maintenance hole in the lower skin panel. The results represent the good agreement with the FEA prediction performed in advance (see Figure 12.26); the error between measured strain and FEA prediction is only 3.0% at highest strain point. The result of visual and non-destructive inspection performed after unloading shows that there was no defect and no detrimental deformation. Thus, the wing box demonstrator has successfully withstood the 100% DLL (Design Limit Load) of 2.5G flight conditions. This fact indicates that the fabricated VaRTM wing box demonstrator has practical acceptability.

References

1) T. Kruckenberg and R. Paton, Resin Transfer Moulding for Aerospace Structures, Kluwer Academic Publishers, Great Britain, 1998.

2) Y. Nagao, T. Nakamura, J. Nakamichi and T. Ishikawa, Low-Cost Composite Manufacturing Technology Development Program in JAXA, Proceedings of the Ninth Japan International SAMPE symposium, Tokyo, Japan, 2005.

12.6 STRUCTURAL HEALTH MONITORING

12.6.1 Detection of Arrested Crack for Foam Core Sandwich Structures Using Optical Fiber Sensors Embedded in a Crack Arrester

Shu Minakuchi*, Ippei Yamauchi*, Nobuo Takeda*, Yasuo Hirose**

* The University of Tokyo

** Kawasaki Heavy Industries, Ltd. (KHI)

Carbon fiber reinforced plastic (CFRP) has been used for almost all modern commercial aircrafts as a primary structural material. However, the potential capability of CFRP cannot be maximized under the conventional structural design concept, consisting of skins, stringers and frames. One of the innovative structural concepts is a foam core sandwich panel structure[1)]. The integral construction consists of two thin facesheets and a lightweight foam core, and can considerably reduce the weight and the number of parts compared to conventional structures. However, it has been pointed out that the crack propagation along the interface between the facesheet and the core is the critical issue. The interface crack originates from the non-visible impact damage or the fatigue shear cracks in the foam core, and seriously degrades the structural integrity. In this context, a crack arrester (Figure 12.27) has been developed by

Hirose et al. [2]. The crack arrester has semi-cylindrical shape and is inserted into the interface. When the crack approaches the arrester, it decreases an energy release rate at the crack tip by suppressing local deformation around the crack. The suppression of the crack propagation has been evaluated under various loading conditions, confirming that the crack arrester can dramatically improve damage tolerance of the foam core sandwich structures. In view of practical use, the arrested crack must be instantaneously detected and appropriate measures need to be taken against the damaged area in order to maintain the structural reliability. However, the crack below the facesheet is difficult to detect using conventional non-destructive inspection techniques. This study proposes an innovative crack detection technique using two fiber Bragg grating (FBG) sensors embedded at both edges of the arrester (Figure 12.28). The change of the strain distribution at the arrester edges induced by suppressing the local deformation around the crack is evaluated using reflection spectra from the FBG sensors. When the interface crack gets close to the crack arrester, the spectrum from the FBG sensor at crack side splits into two peaks due to the birefringence effect of the FBG sensor [3]. On the other hand, the spectrum from the FBG sensor opposite to the crack does not change. This is because only the arrester edge at the crack side contributes to the crack suppression. Thus, the arrested crack can be detected comparing reflection spectra from the two FBG sensors. In this study, we began by evaluating the validity of the proposed technique through numerical simulation. Finite element analysis (FEA) was conducted on double cantilever beam (DCB) and end-notch flexure (ENF) foam core sandwich specimens and the changes in the reflection spectra induced by suppressing the Mode I and Mode II type cracks were predicted. As the crack approached to the arrester, the reflection spectrum from the FBG sensor at the crack side clearly split into two peaks. On the other hand, the reflection spectrum from the FBG sensor opposite to the crack hardly changed. Hence the crack could be detected by comparing reflection spectra from the two FBG sensors. It was also revealed that the facesheet bending and the in-plane core deformation played important roles in arresting the interface crack and consequently introduced the spectral changes. Finally, we conducted verification tests. The measured spectra corresponded well with the analysis results and the crack detection technique was validated. The proposed technique enables an effective application of the crack arrester and significantly improves the reliability of the foam core sandwich structures.

References

1) P. C. Zahlen, M. Rinker and C. Heim, "Advanced manufacturing of large complex foam core sandwich panels," *Proceedings of the 8th International Conference on Sandwich Structures (ICSS8)*, pp. 606-623 (2008).

2) Y. Hirose, M. Hojo, A. Fujiyoshi and G. Matsubara, "Suppression of interfacial crack for foam core sandwich panel with crack arrester," *Adv. Composite Mater.* 16(1), pp. 11-30 (2007).
3) R. Gafsi and M. A. El-Sherif, “Analysis of induced-birefringence effects on fiber Bragg gratings,” *Optical Fiber Technology* 6 (3), pp. 299-323 (2000).

12.6.2 Development of SHM System to Evaluate De-bonding in Composite Adhesive Structures

Hideki Soejima*, Noritsugu Nakamura*, Toshimichi Ogisu*, Hiroshi Wakai*, Yoji Okabe**, Nobuo Takeda**, and Yasuhiro Koshioka#

* Fuji Heavy Industries Ltd.

** The University of Tokyo

R&D Institute of Metal and Composites for Future Industries (RIMCOF)

Structure health monitoring (SHM) systems can diagnose the structure integrity on demand by using sensors installed in structures permanently. Because carbon fiber reinforced plastic (CFRP) has excellent mechanical properties which can contribute to reduce structural weight, CFRP is applied to not only secondary structures, but also primary structures of aircraft in recent years. However, it is difficult to assess deterioration of CFRP structures by visual inspection as compared with metallic structures. Therefore design allowable of aircraft is set a level that is higher than the expected level of CFRP in order to ensure safety and reliability of aircraft structures. One of the methods to apply CFRP to aircraft structures with optimum mechanical properties and ensure safety and reliability of structures is to apply the SHM system to aircraft.

In this background, we have developed a novel SHM system that can evaluate debonds of adhesive layers and delaminations in CFRP structures, such as skin/stringers of wing structures. The SHM system consists of PZT transducers, which generate Lamb Waves into the CFRP structures, fiber Bragg grating optical fiber sensors (FBG sensor), which can detect Lamb Waves propagated through CFRP structures, and interrogation device, whose width, depth and height are about 370 mm, 300 mm, and 150 mm respectively. The diameter of the FBG sensor used in the SHM system is about 50 μm, which is smaller than standard optic fiber. Therefore mechanical properties of CFRP don’t degrade even if the FBG sensor is embedded in CFRP laminate or integrated into adhesive line. A PZT actuator and FBG sensor are installed in a part which has to be inspected. When debonds or delaminations are generated in the propagating path of Lamb Waves, Lamb Waves detected by the FBG sensor

change shown in Figure 12.29. The SHM system can evaluate the structure integrity by detecting and analyzing the change of Lamb Waves.

We conducted sub-component test in order to evaluate the detecting capability of the SHM system. Figure 12.30 shows the sub-component test article which simulated CFRP skin/stringer bonding structure. FBG optical fiber sensors were bonded to the surface of stringers by adhesive and integrated into adhesive lines between stringers and skin. PZT actuators were bonded to the same surface of the skin to which the stringers were bonded. Debonds and delaminations were introduced to the bonded sections of skin/stringer by impacts. Some impacts were introduced to the same point with different energy levels. In order to identify the damaged area, we conducted the A-scan which is generally applied to inspection of CFRP structures. We evaluated the detecting capability of the SHM system by comparing results of the SHM system with the results of the A-scan. Figure 12.31 shows the results of the inspection by A-scan. The damaged area increases as the number of impact increases. In the SHM system, correlation coefficients are derived from detected Lamb Waves to evaluate the change of detected Lamb Waves quantitatively. Figure 12.32 shows examples of Lamb Waves detected by the SHM system. The waveforms of Lamb Waves have changed as the number of impact increases. Figure 12.33 shows the relationship between correlation coefficient and damaged areas identified by A-scan. The correlation coefficient decreases gradually as the damaged area increases.

As a result, it was verified that the SHM system could evaluate the damaged area by the correlation coefficient derived from Lamb Waves.

12.6.3 Research and Development of Impact Damage Detection System for Airframe Structures using Optical Fiber Sensors

Hiroaki Tsutsui*, Noriyoshi Hirano*, Junichi Kimoto*, Takahiko Akatsuka*, Hirofumi Sashikuma*, Naoyuki Tajima*, Nobuo Takeda**

* Kawasaki Heavy Industries, Ltd. (KHI)

** The University of Tokyo

Carbon fiber reinforced plastic (CFRP) composites have been used extensively for light weight airframe structures because of their high specific strength and stiffness. Because of the serious decrease in composites caused by damage, compression after impact (CAI) strength is regarded as an important design criterion. As a damaged part should be inspected in detail by traditional non-destructive inspection (NDI) methods, such as ultrasonic C-scan and soft

X-ray, the part has to be removed from operational airframe structures usually at great expense in both labor and downtime.

We aim at the aircraft application of our impact damage detection (IDD) system for composite airframe structures, as shown in Fig. 12.34. The IDD system consists of a composite structure with installed optical fiber sensors and a monitoring measurement system. We utilize two types of measurements for impact damage detection using optical fiber sensors, as shown in Fig. 12.35. One of them is an optical loss measurement. When an optical fiber is subjected to damage, local bending by impact damage, such as delamination and matrix cracking, the optical intensity of the optical fiber decreases. The initiation of damage can be judged from the degree of the optical loss. The other is a strain measurement using a Fiber Bragg Grating (FBG) sensor. This sensor can measure the strain induced by impact events. The initiation of damage can be also judged from the change in strain responses, and the damage position can be detected using the difference of the arrival time of the strain to each sensor.

In FY 2002, we have carried out the development and demonstration of the IDD technologies for composite structures[1), 2)], as shown in Fig. 12.36. As the result, it was confirmed that the system could detect barely visible impact damage (BVID) in composite structures. This system can be used for in-flight damage detection as well as for on-ground damage detection, and expected to provide cost reduction for inspection and associated work.

To get the prospect of aircraft application of the IDD system is a target of this development from FY 2006. For the application to a practical airframe, the durability of the system should be confirmed. As the first step, several coupon level composite specimens with embedded small-diameter optical fibers were subjected to cyclic loading. The effect of the embedment on the mechanical properties of the composites and the optical intensity of the optical fibers was investigated. Then a system evaluation test using a stiffened panel (Fig. 12.37) with 3 blade type stringers was carried out. The panel with 1,800mm in length and 500mm in width has 13 small-diameter optical fiber sensors including 4 FBG sensors. Those sensors are embedded in the skin, stringer and interlaminar region of the skin/stringer. The panel was subjected to several impact loading before and after compressive cyclic loading test as shown in Fig. 12.38. In the test, the durability of the damage detection function was estimated. It was confirmed that a damaged part and an impact point were detected as shown in Fig. 12.39.

This work was conducted as a part of the project, “ Civil Aviation Fundamental Technology Program-Advanced Materials & Process Development for Next-Generation

Aircraft Structures ” under the contract with RIMCOF, funded by Ministry of Economy, Trade and Industry (METI) of Japan.

References

1) Tajima N., Sakurai T., Sasajima M., Takeda N. and Kishi T., “Overview of the Japanese Smart Materials Demonstrator Program and Structures System Project”, Adv. Composite Mater., 13(1), pp. 3-15 (2004).

2)Tsutsui H., Kawamata A., Kimoto J., Isoe A., Hirose Y., Sanda T. and Takeda N., “Impact damage detection system using small-diameter optical-fiber sensors embedded in CFRP laminate structures”, Adv. Composite Mater., 13(1), pp. 43-55 (2004).

12.6.4 Full-Field Damage Detection System for Composite Structures Using Pulse-Laser Generated Lamb Waves

Ichiya Takahashi and Nobuo Takeda

Department of Aeronautics and Astronautics, The University of Tokyo

Takatsubo et al.[1)] has recently developed a laser scanning method for the visualization of ultrasounds propagating on a three-dimensional object with an arbitrary shape. A pointed pulsed laser is ejected on the surface of a structure which generates Lamb waves in the structure due to induced transient thermal stresses. The Lamb waves are detected by an AE sensor placed on the structure. The pointed pulse laser is scannnd in the surface plane of the structure and dynamic strain data are instantaneously stores in a digital memory along with the position data of the incident pulse. These data can be analyzed to reconstruct the full-field Lamb wave propagation initiating from the position of the AE sensor and to detect the damage in the structure. This technique is most suitable for on-site impact damage detection in curved and complex composite structures (Fig. 12.40). The effects of anisotropic elastic moduli should be well taken care of in order to analyze the strain data. Figure 12.41 presents visualized Lamb wave (50 kHz and 300 kHz) propagation along with C-scanned images of impact-induced delamination patterns in quasi-isotropic composite laminates. Figure 12.42 also provides the detected impact-induced delamination in repaired quasi-isotropic composite laminates.

1) Takatsubo et al., *Trans. of the Jpn Soc. of Mech. Eng., Series A*, 72(718), pp. 945-950, (2006).

12.7 AIRCRAFT ACCIDENT INVESTIGATION

12.7.1 Aircraft Accident Investigation and Aircraft Serious Incident Investigation

Ikuo Takagi
Japan Transport Safety Board (JTSB)

(1) Total number of registered aircraft in Japan

As of December 31, 2008, the number of registered civil aircraft in Japan was 2,664. This accounts for 1,228 airplanes (of which 582 airplanes with reciprocating engines), 768 helicopters, 665 gliders inclusive of motor gliders and 3 airships.

(2) Statistics in relation to the accident and serious incidents investigation

The number of accidents and serious incidents which JTSB investigated in the past two years are shown in Tables 12.5 and 12.6. Of the total 57 occurrences, 27 are still under investigation. Of the 30 published accident/incident investigation reports, pilot and maintenance related causes accounted for 53% and 7% respectively. Other causes such as weather conditions or undetermined, accounted for remaining 40%.

(3) Fatigue failure related serious incident

a. Summary of the serious incident

A Boeing 737-500 landed New Chitose Airport on November 20, 2006, at 21:13 JST. At about 21:16 JST, after starting the Auxiliary Power Unit (APU) during taxing to spot, APU fire warning was indicated in the instrument panel. Therefore, the flight crew stopped the airplane in taxi way, and activated the APU's fire extinguisher system.

As a result of inspection, it was found that the cause of APU fire was fracturing of clasps (coupling) which fixed the combustion chamber to turbine section of APU. (See Figure 12.43)

b. fractured clasp(coupling)

The clasp (coupling) was made of stainless steel, about 22 millimeters wide, 1 millimeter thick, belt-like shape. The edge of clasp (coupling) is turned over to install tightening clasp, and the edge of clasp (coupling) is spot-welded. Fracture originated around the location of spot welding. (See Figure 12.44)

(Supplement: Spot welding is the way for joining two metal sheets by melting and solidifying for turning on electricity under pressure across a pair of copper alloy electrodes.)

c. Cause of fracture

As a result of fractographic investigation of fracture surface of the clasp (coupling), it was estimated that some cracks had originated around the location of spot welding, and the cracks has grown by longtime repeated load, and finally the clasp (coupling) has been fractured. The cause of generating cracks around the location of spot welding, was considered

possible that there was any cause in the spot welding at the time of manufacturing of the clasp (coupling). This, however, could not be confirmed.

12.8 ICAF DOCUMENTS DISTRIBUTED BY JAPAN DURING 2007 TO 2009

(1) H. Terada, and T. Okada, Problems of Laboratory Tests for Durability Evaluation of Full-Scale Structures, to be published in Int. J. Fatigue, 2009.
(2) Y. Hirose, M. Hojo, A. Fujiyoshi and G. Matsubara, "Suppression of interfacial crack for foam core sandwich panel with crack arrester," Adv. Composite Mater. Vol. 16, No. 1, 2007, pp. 11-30.
(3) S. Takeda, Y. Yamamoto, Y. Okabe and N. Takeda, “Debonding Monitoring of Composite Repair Patches Using Embedded Small-diameter FBG Sensors,” Smart Materials and Structures, Vol. 16, 2007, 763-770.
(4) Y. Okabe, J. Kuwahara, K. Natori, N. Takeda, T. Ogisu, S. Kojima and S. Komatsuzaki, “Evaluation of Debonding Progress in Composite Bonded Structures Using Ultrasonic Waves Received in Fiber Bragg Grating Sensors,” Smart Materials and Structures, Vol. 16, No. 4, 2007, pp. 1370-1378.
(5) A. Yoshimura, S. Yashiro, T. Okabe and N. Takeda, “Characterization of Tensile Damage Progress in Stitched CFRP Laminates,” Advanced Composite Materials, Vol. 16, No. 3, 2007, pp. 223-244
(6) S. Minakuchi, Y. Okabe and N. Takeda, “Segment-Wise Model” for Theoretical Simulation of Barely Visible Indentation Damage in Composite Sandwich Beams: Part I– Formulation,” Composites Part A, Vol. 39, 2008, pp. 133-144.
(7) S. Minakuchi, Y. Okabe and N. Takeda, ““Segment-Wise Model” for Theoretical Simulation of Barely Visible Indentation Damage in Composite Sandwich Beams: Part II – Experimental Verification and Discussion,” Composites Part A, 38, 2008, pp. 2443-2450.

ACKNOWLEDGEMENTS

The editors appreciated the members of the ICAF national committee of Japan Society for Aeronautical and Space Sciences, for their contribution in preparation of this national review and continuing discussion in the committee.